



COLORADO

Department of Transportation

CDOT Applied Research and Innovation Branch



Technical Report Documentation Page

1. Report No.		2. Government Accession No.		3. Recipient's Catalog No.	
4. Title and Subtitle				5. Report Date	
				6. Performing Organization Code	
7. Author(s)				8. Performing Organization Report No.	
9. Performing Organization Name and Address				10. Work Unit No. (TRAIS)	
				11. Contract or Grant No.	
12. Sponsoring Agency Name and Address				13. Type of Report and Period Covered	
				14. Sponsoring Agency Code	
15. Supplementary Notes					
16. Abstract					
17. Keywords			18. Distribution Statement		
19. Security Classif. (of this report)		20. Security Classif. (of this page)		21. No. of Pages	22. Price

The contents of this report reflect the views of the author(s), who is(are) responsible for the facts and accuracy of the data presented herein. The contents do not necessarily reflect the official views of the Colorado Department of Transportation or the Federal Highway Administration. This report does not constitute a standard, specification, or regulation.

Acknowledgement

This material is based upon work supported by the U. S. National Science Foundation National Center for Atmospheric Research, which is a major facility sponsored by the National Science Foundation under Cooperative Agreement No. 1852977. This research was funded by the Colorado Department of Transportation (CDOT) in collaboration with the Colorado Department of Public Health and Environment (CDPHE) under Award No. 2023-0920. Any opinions, findings, and conclusions or recommendations expressed in this material do not necessarily reflect the views of the National Science Foundation, Colorado Department of Public Health and Environment, nor the Colorado Department of Transportation. The authors wish to thank the contributions of CDPHE personnel including Tom Moore and Gordon Pierce (retired), as well as CDOT personnel including Steve Cohn, Curt Frischkorn, Meteb Mejbil, Bryan Roeder, Thien Tran, and Air Sciences Inc. personnel Katie Kolesar and Matt Mavko for their comments and inputs to guide the development of this project.

Table of Contents

Acknowledgement	4
Table of Contents	4
List of Figures	5
Executive Summary	7
Implementation Statement	7
1 Introduction	9
1.1 Study Objectives.....	10
1.2 Background	10
1.3 Scope of Study.....	11
2 Methods	12
2.1 Data	12
2.2 Simulation	12
3 Results	14
3.1 Simulation	14
3.2 Pollutant Concentration Analysis.....	19
3.3 Low-Cost Sensor Analysis	27
3.4 Study Limitations	29
4 Conclusions and Opportunities	30
5 References	32

List of Figures

Figure 1.1 The Interstate-270 corridor study region within the Denver Metropolitan Area.	9
Figure 1.2 Air quality instrument sites along the Interstate 270 corridor study region.	10
Figure 2.1 Two domain WRF-Chem-LES configuration, with the inner domain covering CDOT air quality research project instrument sites along the I-270 corridor.	13
Figure 2.2 Vertical profiles of air temperature (red line), dewpoint temperature (green line), and wind barbs plotted on a Skew-T Log-P diagram. The radiosonde capturing the profiles was launched at 12 UTC on 10 June 2022 from Denver International Airport. This profile is used as the initial condition for the WRF-Chem-LES simulation.	13
Figure 3.1 Horizontal planview of PM _{2.5} concentration in the lowest model grid cell on outer domain (d01) at 2100 UTC (1500 MDT) on 10 June 2022.	15
Figure 3.2 Horizontal planview of PM _{2.5} concentration in the lowest model grid cell on outer domain (d01) at 0000 UTC on 11 June 2022 (1800 MDT on 10 June 2022).	16
Figure 3.3 Horizontal planview of PM _{2.5} concentration in the lowest model grid cell on outer domain (d01) at 0300 UTC on 11 June 2022 (2100 MDT on 10 June 2022).	17
Figure 3.4 Horizontal planview of PM _{2.5} concentration in the lowest model grid cell on outer domain (d01) at 0600 UTC (0000 MDT) on 11 June 2022.	18
Figure 3.5 CDPHE Adams-Birch station PM _{2.5} observed hourly through the study period from 1200 UTC on 10 June 2022 to 0600 UTC on 11 June 2022 (0600 MDT on 10 June 2022 to 0000 MDT on 11 June 2022).	20
Figure 3.6 CDPHE Adams-Birch station PM _{2.5} observed hourly through the study period from 1200 UTC on 10 June 2022 to 0600 UTC on 11 June 2022 (0600 MDT on 10 June 2022 to 0000 MDT on 11 June 2022).	21
Figure 3.7 CDPHE La Casa NCORE (EPA AQS ID: 08-031-0026) station PM _{2.5} observed hourly through the study period from 1200 UTC on 10 June 2022 to 0600 UTC on 11 June 2022 (0600 MDT on 10 June 2022 to 0000 MDT on 11 June 2022).	21
Figure 3.8 PurpleAir Cultivando 25 (I-270 and Platte River) station PM _{2.5} observed at two-minute resolution through the study period from 1200 UTC on 10 June 2022 to 0600 UTC on 11 June 2022 (0600 MDT on 10 June 2022 to 0000 MDT on 11 June 2022).	22

Figure 3.9 PurpleAir Cultivando 14 (I-270 and Quebec Street) station PM2.5 observed at two-minute resolution through the study period from 1200 UTC on 10 June 2022 to 0600 UTC on 11 June 2022 (0600 MDT on 10 June 2022 to 0000 MDT on 11 June 2022). 22

Figure 3.10 PurpleAir Cultivando 7 Vasquez and Swansea site PM2.5 observed at two-minute resolution through the study period from 1200 UTC on 10 June 2022 to 0600 UTC on 11 June 2022 (0600 MDT on 10 June 2022 to 0000 MDT on 11 June 2022). 23

Figure 3.11 Adams Birch EPA site PM2.5 observed hourly (blue/top line) and WRF-Chem-LES simulation output (black/bottom line) through the study period from 1200 UTC on 10 June 2022 to 0600 UTC on 11 June 2022 (0600 MDT on 10 June 2022 to 0000 MDT on 11 June 2022)... 24

Figure 3.12 Globeville EPA site PM2.5 observed hourly (blue/top line) and WRF-Chem-LES simulation output (black/bottom line) through the study period from 1200 UTC on 10 June 2022 to 0600 UTC on 11 June 2022 (0600 MDT on 10 June 2022 to 0000 MDT on 11 June 2022)... 24

Figure 3.13 La Casa NCORE EPA site PM2.5 observed hourly (blue/top line) and WRF-Chem-LES simulation output (black/bottom line) through the study period from 1200 UTC on 10 June 2022 to 0600 UTC on 11 June 2022 (0600 MDT on 10 June 2022 to 0000 MDT on 11 June 2022) 25

Figure 3.14 Ratio of PM2.5 construction emissions to total PM2.5 emissions along the corridor from WRF-Chem-LES simulations across the outer domain (d01) through the study period from 1200 UTC on 10 June 2022 to 0600 UTC on 11 June 2022 (0600 MDT on 10 June 2022 to 26

Figure 3.15 Proof-of-concept representation of the WRF-Chem-LES simulations across the inner domain (d02) through the study period from 1200 UTC on 10 June 2022 to 0600 UTC on 11 June 2022 (0600 MDT on 10 June 2022 to 0000 MDT on 11 June 2022) over the I-270 highway to show dispersion from the line source of emissions. 27

Figure 3.16 Low-cost PM2.5 sensors within the high-resolution spatial and temporal model domain (Figures 1.2 and 2.1) showing the hourly mean +/- one standard deviations. 28

Figure 3.17 Co-located sensors and their time series along the I-270 corridor. 29

Executive Summary

Understanding construction emissions and their impacts to air quality is a shared responsibility. The Colorado Department of Transportation (CDOT) and the Colorado Department of Public Health and Environment (CDPHE) have pooled resources to better quantify and understand the influence of construction activities on air quality. The objective of this pilot study is to explore the feasibility of modeling the impact of construction activities along the Interstate-270 corridor on air quality in the Denver metro area. Given the small scales (a few meters) necessary for this study, the Weather Research and Forecasting model coupled with Chemistry in the Large-Eddy Simulation (WRF-Chem-LES) mode, which can resolve atmospheric turbulence down to 10 m, is used. WRF-Chem-LES is implemented in a quasi-idealized configuration representative of synoptically quiescent summertime meteorological conditions in the Denver metro area. Emissions (e.g., VOCs, PM_{2.5}) related to construction activities are defined in consultation with CDOT and CDPHE. Additionally, low-cost air quality sensors are leveraged along/near the corridor to consider potential opportunities to implement model bias correction. The primary focus of the analysis was PM_{2.5} construction emissions. Overall, it was found that the model was capable of simulating construction emissions; however, there was a noteworthy low bias relative to observed PM_{2.5} emissions. This is likely a result of the thickness of the model lowest level relative to the sensor measurement height. An assessment of CDOT/CDPHE deployed low-cost sensors relative to other data available along/near the Interstate-270 corridor demonstrated reasonable consistency in the overall trend of the data, albeit noteworthy differences were attributable to different temporal resolutions and sensor placement. Future work can build upon and further refine this modeling framework as well as identify opportunities to prioritize sensor placement and future modeling studies.

The model simulations demonstrate the feasibility and capability of capturing the fate of synthetic construction emissions used (i.e., 30% above background emissions for a quiescent study day) along a roadway corridor under idealized model conditions. There are several important limitations in the current study including the lack of actual construction activities along the corridor, the singular study period day, the quasi-idealized model configuration, the limited tracer selection, the lack of active chemistry in the model simulations, and the time and resource constraints of the project. Nevertheless, this work is a foundation for further development of the modeling framework once construction activities are occurring along the corridor as well as expansion to other regions with construction activity. It also represents an initial demonstration of the capabilities a sophisticated meteorological model (WRF-Chem-LES) when applied to the study of transportation construction air quality. This pilot study employs an interdisciplinary approach to better understand and quantify transportation-related emissions.

Implementation Statement

As a pilot study, the primary outcome of this work is to inform decisions about further research, including directions and situations where such research could be applied. As described in the body of this report, there are opportunities for further development of the WRF-Chem-LES model for construction air quality uses, and for its application more generally to address transportation air quality research questions. These include taking advantage of its reactive chemistry capability and analyzing tracers and chemicals in addition to the PM_{2.5}. Further opportunities are to consider vehicular dust entrainment, more realistic inclusion of surface roughness parameters, and driving the model with actual measured construction emissions. More

ambitious extensions would be to couple the WRF-Chem-LES modeling framework with the EPA Motor Vehicle Emissions Simulator (MOVES; EPA 2022) which would allow for a more detailed assessment of vehicular emissions in the context of atmospheric and chemical dynamics.

1 Introduction

The Colorado Department of Transportation (CDOT) has partnered with the Colorado Department of Public Health and Environment (CDPHE) to measure, quantify, and understand the contributions of road maintenance and construction activities to air quality, pollution, and dispersion along and near roadways across the state. The focus of the current assessment is along the Interstate-270 corridor, hereafter referred to as the “corridor”, through the Denver Metropolitan Area (Figure 1.1). CDOT has planned substantial improvements to ease congestion, promote safety, and improve the quality of life along the corridor once the work has been completed (CDOT 2022). To understand the potential air quality impacts during construction activities, CDOT and CDPHE have deployed a network of air quality sensors along the corridor (Figure 1.2). These observations enable a more refined understanding of air quality impacts along the corridor before, during, and after the planned construction activities.

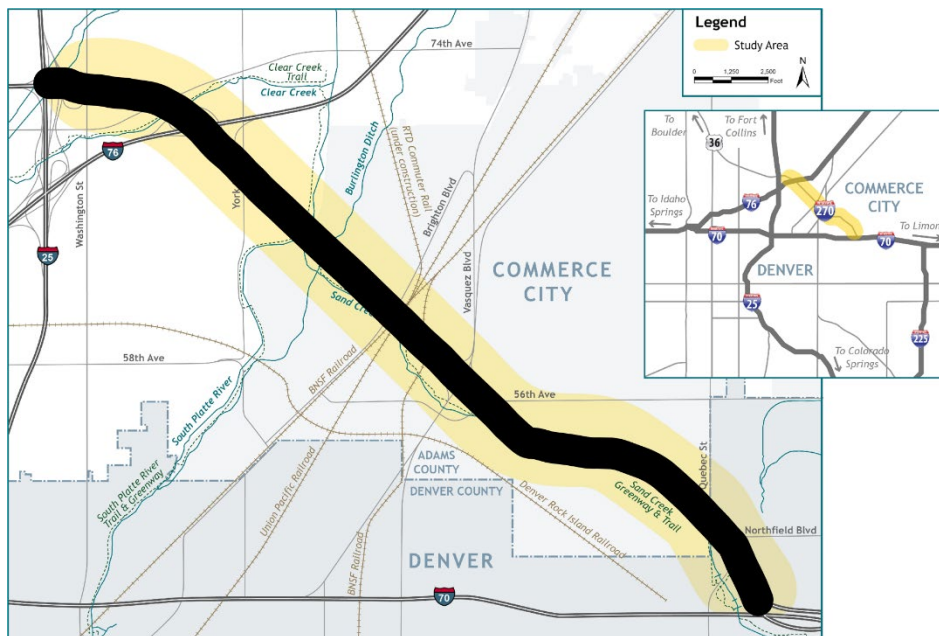


Figure 1.1 The Interstate-270 corridor study region within the Denver Metropolitan Area.

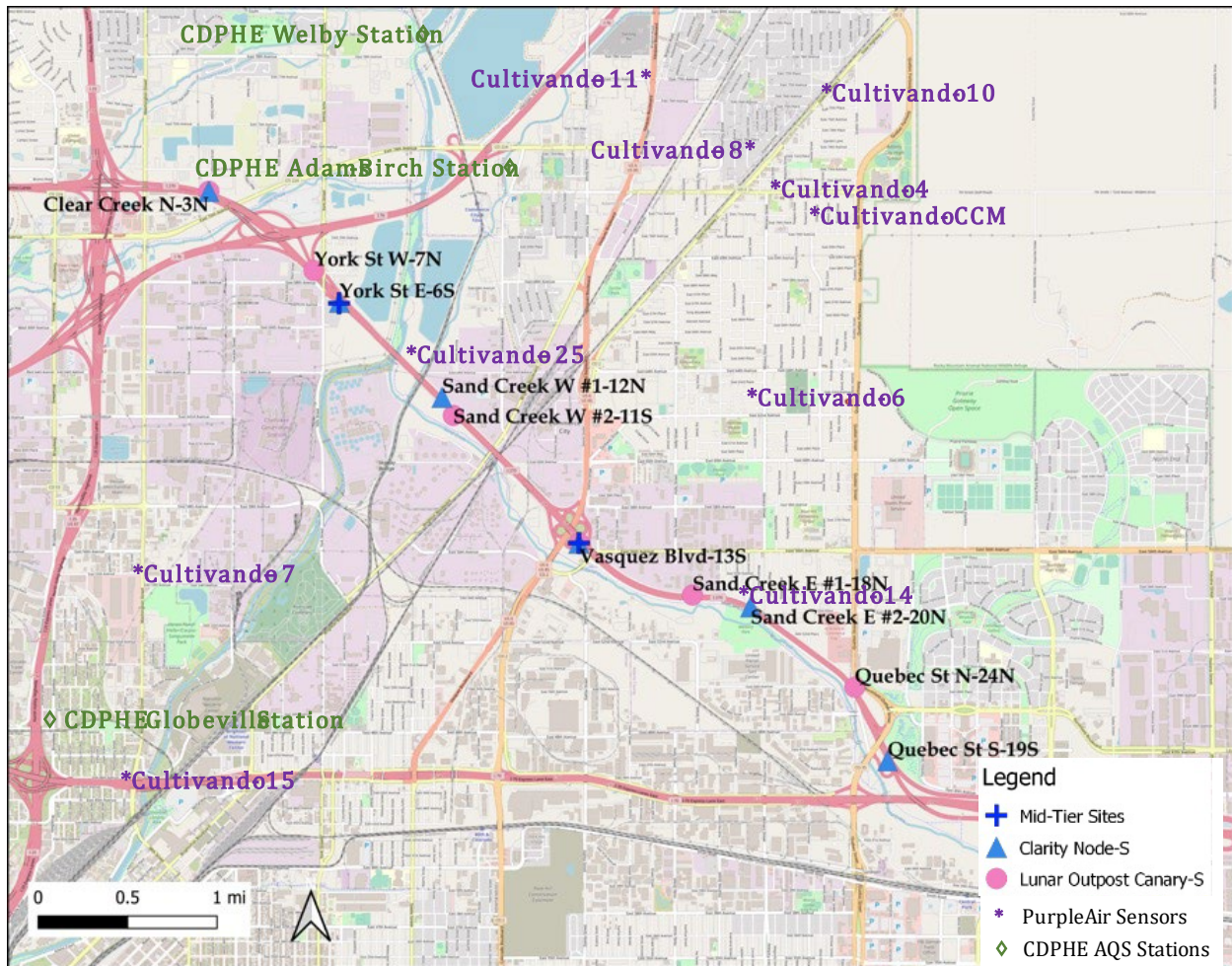


Figure 1.2 Air quality instrument sites along the Interstate 270 corridor study region.

1.1 Study Objectives

The objective of this pilot study is to explore the feasibility of modeling the impact of simulated construction activities along the corridor on air quality in the Denver metro area with a sophisticated, high-resolution meteorological model that includes particulate and chemical tracers. Additionally, this pilot study leveraged different types of air quality sensors along the corridor to evaluate model simulations with the eventual goal of employing less expensive sensors for measurements to better quantify air quality impacts.

1.2 Background

Air pollution poses substantial health hazards to communities (Pope and Dockery 2012). In the atmospheric boundary layer, the lowest layer of the atmosphere that most influences air quality, transportation research applications have focused on air pollution and turbulent transport modeling to understand dispersion of pollutant concentrations and emission reductions. Additional complexity includes the impact of vehicles themselves (for example their wakes) on dispersion and turbulent transport of pollutants.

The atmospheric boundary layer is the region of the atmosphere that directly influences daily societal operations – it is the layer in which we live. Within the atmospheric boundary layer,

there can exist several unique internal boundary layers. The urban boundary layer (Loughner et al. 2012; Barlow 2014) contains the densest human populations, yet it remains one of the lesser understood microclimates. Within the urban boundary layer, roadways represent a microscale feature that are difficult, but imperative, to explicitly consider. From a public health perspective, air pollution, particularly vehicular emissions, pose significant and long-term health concerns worthy of further study (Kunzli et al. 2000; Pope and Dockery 2012).

Relevant research has focused on quantification and mitigation of air pollution in the immediate vicinity of the roadway (Turner 1970; Ragland and Peirce 1975; Zimmerman and Thompson 1975; Heist et al. 2009; Durant et al. 2010; Mao et al. 2013; Pournazeri and Princevac 2015). Historical studies (e.g., Ragland and Peirce 1975) have considered a theoretical modeling approach to quantify the variability in air pollutant concentrations near roadways due to highway traffic. More recent work (e.g., Heist et al. 2009; Durant et al. 2010) has performed practical, in-situ observational-based assessments. Further studies (e.g., Eskridge and Hunt 1979; Gordon et al. 2012) have attempted to consider the individual influence of vehicular wake turbulence and traffic flow on turbulent kinetic energy and subsequent air pollution dispersion. Modeling and observational assessments both address a critical need to promote public safety and mitigate the impacts of air pollution from vehicular emissions. These studies make clear the wide range of scales that models must address, from resolving roads a few tens of meters across or vehicle wakes (microscale), to horizontal ranges many tens of km across (mesoscale) and vertical scales of a few meters or less near the surface to several km throughout the atmospheric boundary layer.

Roadway configuration (e.g., grade level, elevated, trench) and adjacent barriers (e.g., shelterbelt or rows of trees used as wind breaks, sound walls) have implications for air pollution, turbulent transport, and dispersion (Heist et al. 2009; Mao et al. 2013; Pournazeri and Princevac 2015). Earlier work (e.g., Ragland and Peirce 1975) assumed the roadway to be at grade level and completely open. Heist et al. (2009) considered the effects of 12 different roadway configurations on pollutant dispersion and use a standard logarithmic velocity profile to assess roughness length, displacement height, and friction velocity for each. Their results suggest that grade level and elevated roadway configurations can result in the greatest amount of downwind pollutant dispersion. Depressed roadway configurations limit downwind pollutant transport; however, they allow for greater recirculation along the roadway itself which yields substantial increases in localized, near-roadway pollutant concentrations. The presence of barriers produced similar results to the depressed roadway configuration. Mao et al. (2013) solely considered the influence of shelterbelt on road dust dispersion for an at-grade level roadway. Their findings were consistent with the previous wind tunnel study (Heist et al. 2009). While shelterbelt did diminish downwind concentrations of the largest dust particles, there was an observed increase in the suspension time of finer dust particles attributable to the recirculation effect. Lastly, Pournazeri and Princevac (2015) considered the influence of sound wall barriers on pollutant dispersion and confirmed that the dominant flow pattern was associated with the recirculation induced by the barriers. While this recirculation, and subsequent turbulent mixing, could lower downwind concentrations, it also had the potential to create localized higher concentrations that could ultimately be transported by changing wind directions.

1.3 Scope of Study

This analysis leverages both a modeling and observational assessment to understand and quantify the potential influence of construction activities on air quality. The model used in this analysis is

the Weather Research and Forecasting model coupled with chemistry in the large-eddy simulation mode (WRF-Chem-LES; Grell et al. 2005; Skamarock et al. 2008; Liu et al. 2011; Powers et al. 2017), which can resolve atmospheric turbulence down to meter scales. WRF-Chem-LES is implemented for an 18-hour period in a quasi-idealized configuration representative of synoptically quiescent, summertime meteorological conditions along the corridor.

2 Methods

2.1 Data

Air quality data are obtained from Environmental Protection Agency (EPA) reference stations, and low-cost sensors (Clarity Node-S and Lunar Outpost Canary-S) deployed by CDOT and CDPHE along the corridor. Data were also collected from regional PurpleAir low-cost sensors to supplement observations. These data are compared to WRF-Chem-LES model simulations to assess the capability of model simulations to capture air quality impacts. The model simulations are described in the section below.

2.2 Simulation

The WRF-Chem-LES model is used within a quasi-idealized framework to examine the diurnal evolution of transport and dispersion of chemical tracers for the 10–11 June 2022 period. This period is selected due to relatively quiescent atmospheric conditions to control for other influences on dispersion. We focus on the period from 12 UTC on 10 June to 06 UTC on 11 June (0600 MDT on 10 June to 0000 MDT on June 11). We use a nested, two-domain configuration, with the outer (d01) and inner (d02) domains resolving turbulence at horizontal grid cell spacing, $dx = 90$ m and 10 m, respectively (Figure 2.1). The vertical grid spacing, dz , is constant at 30 m, with a grid top set to 3 km. We impose periodic boundary conditions in the x and y directions on d01, while d02 has open boundary conditions in x and y , allowing for a smooth evolution of atmospheric boundary layer features. A time step of 1 second is used for the outer domain, while a time step of 1/9 second is used for the inner domain to align with the 1:9 parent-child grid spacing ratio. The outer domain is run for the entire 18-hour period, and the inner domain is activated for the final four hours (02–06 UTC on 11 June, corresponding to 2000 to midnight MDT) to examine the afternoon-to-evening transition period, specifically related to shifts in atmospheric structure and transportation emissions. During this transition, we expect that chemical tracers will accumulate more at the surface due to a reduction in vertical mixing as solar heating diminishes.

The initial vertical meteorological conditions (Figure 2.2) are provided by a radiosonde launched at the Denver International Airport at 12 UTC on 10 June, corresponding to the start time of our simulation. The initial wind profile is assumed to be in geostrophic balance. As the simulation evolves, the wind deviates from geostrophic balance due to frictional forces and the development of turbulence. Note that the large-scale forcing (imposed via the geostrophic wind) is assumed to be constant throughout the simulation due to its relatively short duration. This assumption is reasonable given the relatively weak synoptic scale forcing on this day. To mimic the diurnal cycle, a time-varying (hourly) horizontal lower boundary condition of surface skin temperature is imposed using the closest model grid cell from the ERA5 model (Hersbach et al. 2020). We allow the WRF-Chem-LES model to compute interactive surface fluxes using the revised MM5 surface layer scheme (Jimenez et al. 2012). No other model physics are activated.

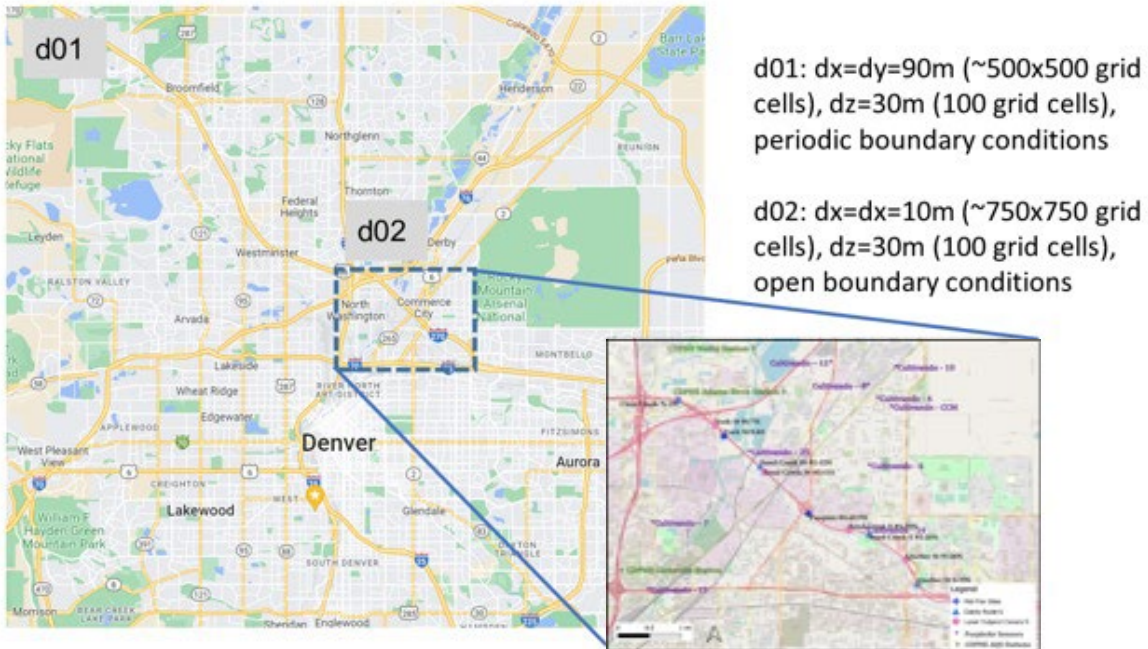


Figure 2.1 Two domain WRF-Chem-LES configuration, with the inner domain covering CDOT air quality research project instrument sites along the I-70 corridor.

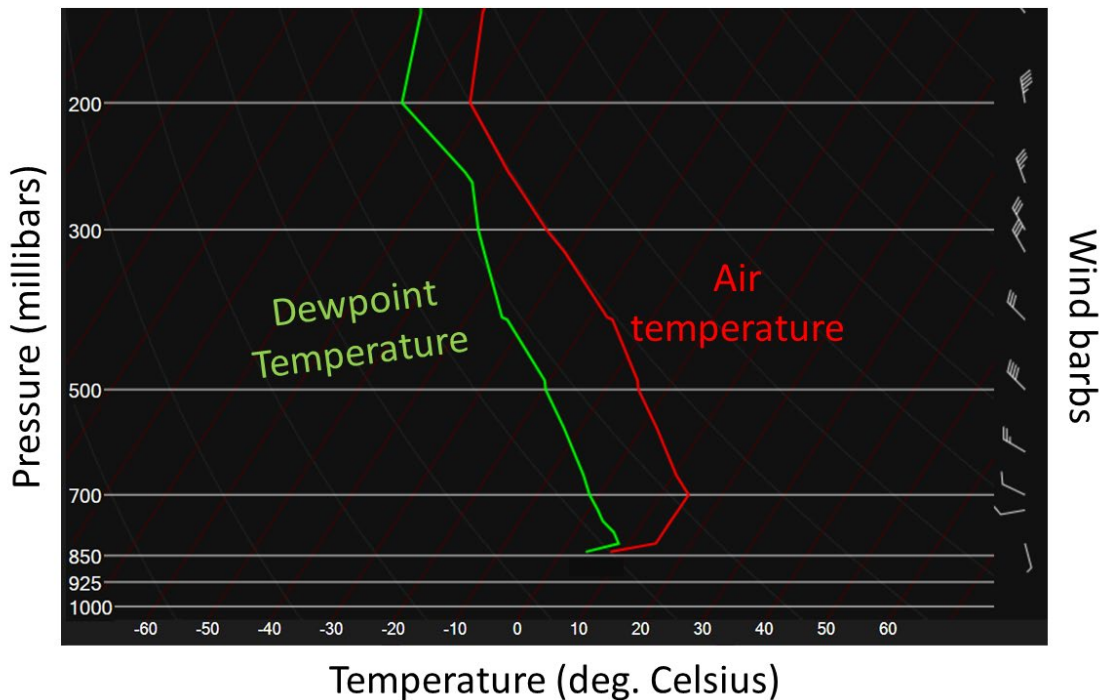


Figure 2.2 Vertical profiles of air temperature (red line), dewpoint temperature (green line), and wind barbs plotted on a Skew-T Log-P diagram. The radiosonde capturing the profiles was launched at 12 UTC on 10 June 2022 from Denver International Airport. This profile is used as the initial condition for the WRF-Chem-LES simulation.

To address the main objectives of this study related to chemical tracer transport and dispersion, we activate four anthropogenic tracers in the model: PM_{2.5}, PM₁₀, toluene, and benzene. The emissions for these chemicals are mapped to the LES domains from the 2017 National Emissions Inventory (NEI; EPA 2021) database at 12 x 12 km² resolution using a mass-conserving approach. These emission rates, which are available at a temporal frequency of one hour, are computed offline prior to the simulation. In addition to these four constituents, we also include two tracers – PM_{2.5}_{construction} and PM₁₀_{construction} – related to construction activities along the I-270 corridor. Construction activity was not present during the proposed simulation period and this pilot study used a proxy of 30% of the PM_{2.5} and PM₁₀ emissions along the corridor as representative of some level of construction emissions. This provides a reasonable and sufficient signature for the model to evaluate the impact of these added emissions throughout the domain as a simplified version of emissions in this proof-of-concept framework.

3 Results

3.1 Simulation

The model simulations (Figures 3.1–3.4; Table 3.1) allow for an understanding of both the spatial and temporal (diurnal) evolution of background concentrations, localized emissions, and construction emissions along the corridor. The model domain represents a fairly complex situation, with many stationary, industrial emission sources. Figures 3.1–3.4 show how the PM_{2.5} concentration near the surface (the lowest model level) evolves at 3-hour intervals through the afternoon and evening transition. For PM_{2.5} during the afternoon, when the boundary layer is well-mixed (Figure 3.1), point sources appear as localized areas of higher concentrations with relatively localized downstream dispersion and entrainment above the lowest level. As the daytime heating begins to weaken, the boundary layer becomes less well-mixed (Figure 3.2), leading to greater low-level horizontal dispersion of PM_{2.5} as well as higher near-surface accumulation of background emissions. Into the evening (Figure 3.3), there is an apparent wind shift from a westerly to more northwesterly direction resulting in further horizontal dispersion and point sources becoming less apparent, and surface concentrations continue to increase. In the final time step (Figure 3.4), there is substantial downstream (i.e., southeasterly) dispersion of PM_{2.5} emissions likely due to boundary layer turbulence and wind shift, with the particulates staying concentrated near the surface. In addition to PM_{2.5}, our simulations also included PM₁₀ and VOCs Benzene and Toluene as tracers to reflect oil and gas industry emissions and traffic emissions, respectively. Table 3.1 provides links to animations of all tracers. The chemical tracers also depict spatial and temporal evolution consistent with their expected patterns of pollutant formation and fate representative simulation day.

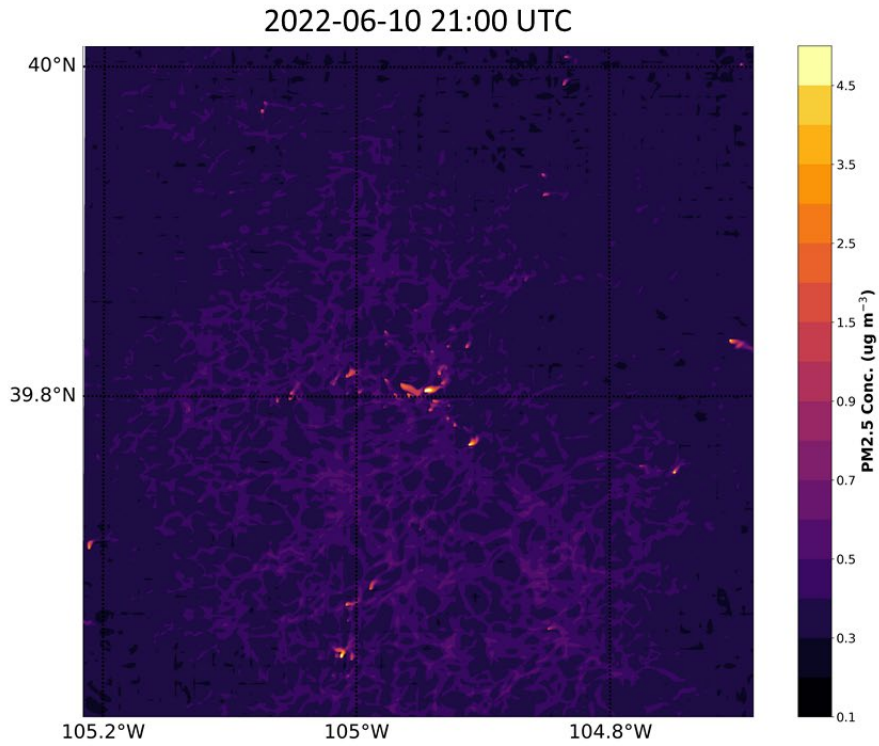


Figure 3.1 Horizontal planview of PM_{2.5} concentration in the lowest model grid cell on outer domain (d01) at 2100 UTC (1500 MDT) on 10 June 2022.

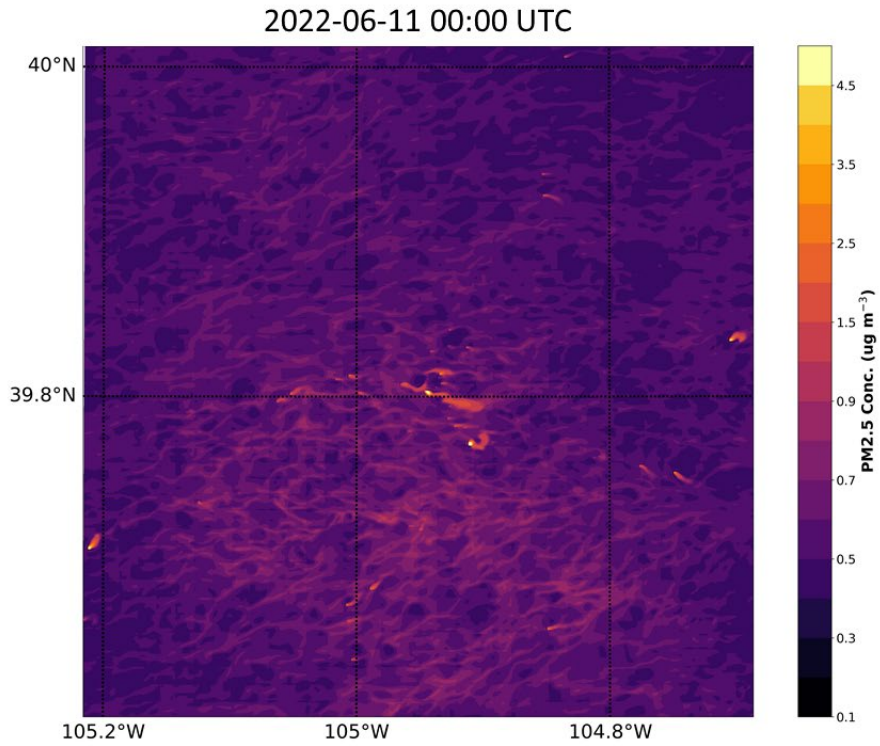


Figure 3.2 Horizontal planview of PM_{2.5} concentration in the lowest model grid cell on outer domain (d01) at 0000 UTC on 11 June 2022 (1800 MDT on 10 June 2022).

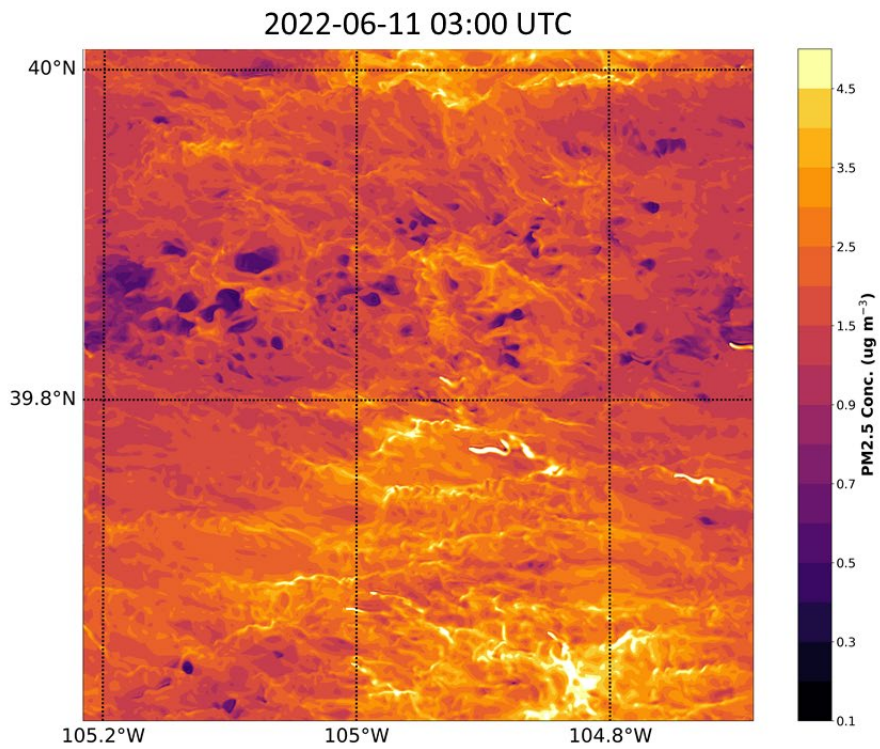


Figure 3.3 Horizontal planview of PM2.5 concentration in the lowest model grid cell on outer domain (d01) at 0300 UTC on 11 June 2022 (2100 MDT on 10 June 2022).

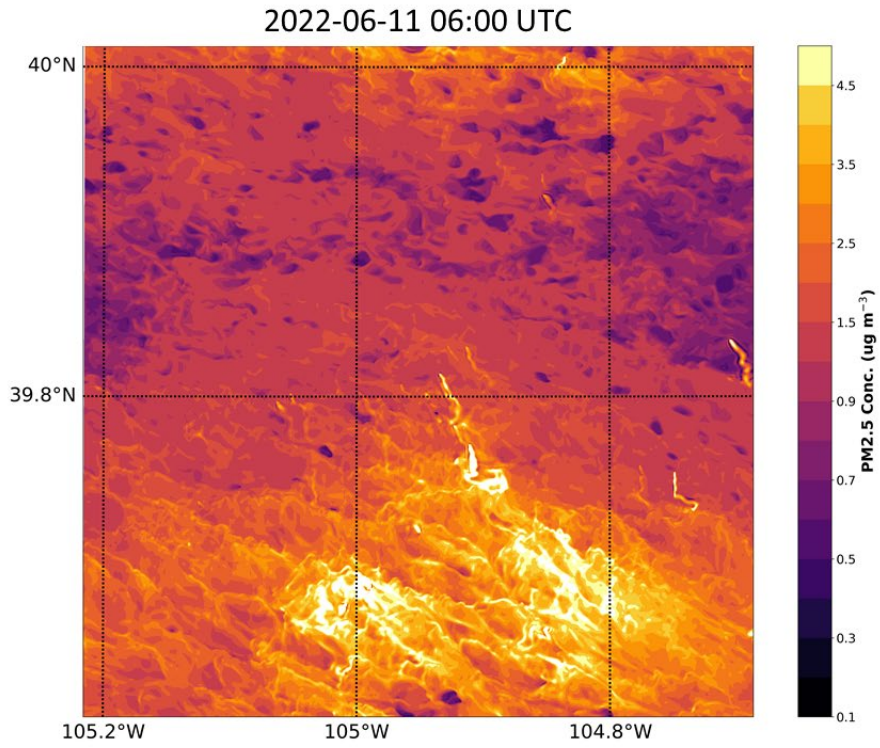


Figure 3.4 Horizontal planview of PM2.5 concentration in the lowest model grid cell on outer domain (d01) at 0600 UTC (0000 MDT) on 11 June 2022.

The following links contain animations for the particulate and chemical traces on the outer (d01) and inner (d02) model domains:

- Outer Domain, PM2.5: https://storage.googleapis.com/cdot-adap-public/dtd/arib/2024_NCAR_Modeling_Road_Construction_Air_Quality_Animations/d01_pm25_contourf_anim.gif
- Outer Domain, PM10: https://storage.googleapis.com/cdot-adap-public/dtd/arib/2024_NCAR_Modeling_Road_Construction_Air_Quality_Animations/d01_pm10_contourf_anim.gif
- Outer Domain, Benzene: https://storage.googleapis.com/cdot-adap-public/dtd/arib/2024_NCAR_Modeling_Road_Construction_Air_Quality_Animations/d01_benz_contourf_anim.gif
- Outer Domain, Toluene: https://storage.googleapis.com/cdot-adap-public/dtd/arib/2024_NCAR_Modeling_Road_Construction_Air_Quality_Animations/d01_tol_contourf_anim.gif
- Inner Domain, PM2.5: https://storage.googleapis.com/cdot-adap-public/dtd/arib/2024_NCAR_Modeling_Road_Construction_Air_Quality_Animations/d02_pm25_contourf_anim.gif
- Inner Domain, PM10: https://storage.googleapis.com/cdot-adap-public/dtd/arib/2024_NCAR_Modeling_Road_Construction_Air_Quality_Animations/d02_pm10_contourf_anim.gif
- Inner Domain, Benzene: https://storage.googleapis.com/cdot-adap-public/dtd/arib/2024_NCAR_Modeling_Road_Construction_Air_Quality_Animations/d02_benz_contourf_anim.gif
- Inner Domain, Toluene: https://storage.googleapis.com/cdot-adap-public/dtd/arib/2024_NCAR_Modeling_Road_Construction_Air_Quality_Animations/d02_tol_contourf_anim.gif

Table 3.1 Animation download links for particulate and chemical tracers on outer and inner model domains.

3.2 Pollutant Concentration Analysis

Reference and Low-Cost Sensor Measurements

A qualitative comparison of EPA reference stations managed by CDPHE (Figures 3.5–3.7) and regional PurpleAir low-cost sensors (Figures 3.8–3.10) demonstrates the advantages of the localized, higher resolution data. The EPA reference locations capture the general diurnal trend of PM2.5 coincident with morning and, more notably, evening peaks reflective of traffic

conditions (i.e., morning and evening rush hour), and the shallower morning and evening boundary layer depth. The Adams-Birch and Globeville stations are very close to a highway, while the La Casa station is approximately 2 blocks from one (not shown on Figure 1.2 as it is just outside of model domain d02). While the timing of peak concentration does not directly align with the peak of traffic, the increased emissions from evening rush hour traffic volumes combined with a decreasing planetary boundary layer height following the loss of daytime heating can compress and further elevate concentrations. It is also an important caveat that the selected day represents a Friday traffic cycle which is likely unique relative to other week or weekend days. The PurpleAir sensors capture a similar trend albeit with much higher time resolution and thus a noisier profile as well more sensitive to spikes in the data. Given the more notable evening increases in both datasets, this period was selected for further evaluation and comparison with model simulations.

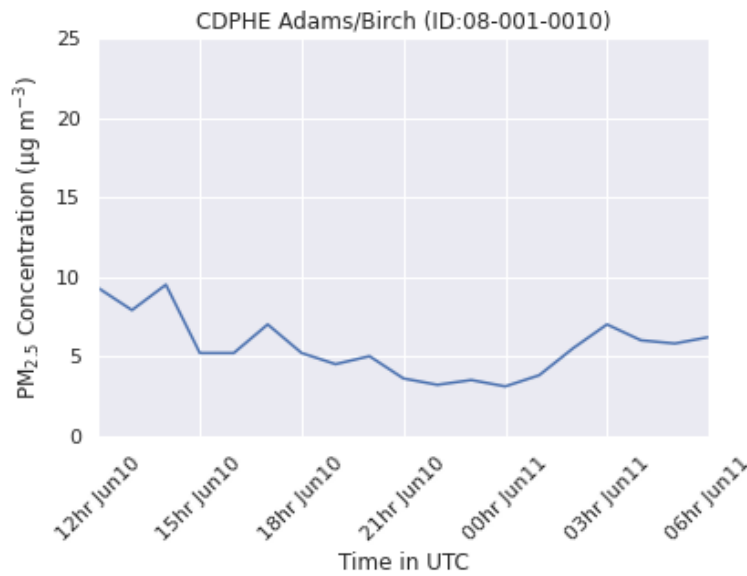


Figure 3.5 CDPHE Adams-Birch station PM_{2.5} observed hourly through the study period from 1200 UTC on 10 June 2022 to 0600 UTC on 11 June 2022 (0600 MDT on 10 June 2022 to 0000 MDT on 11 June 2022).

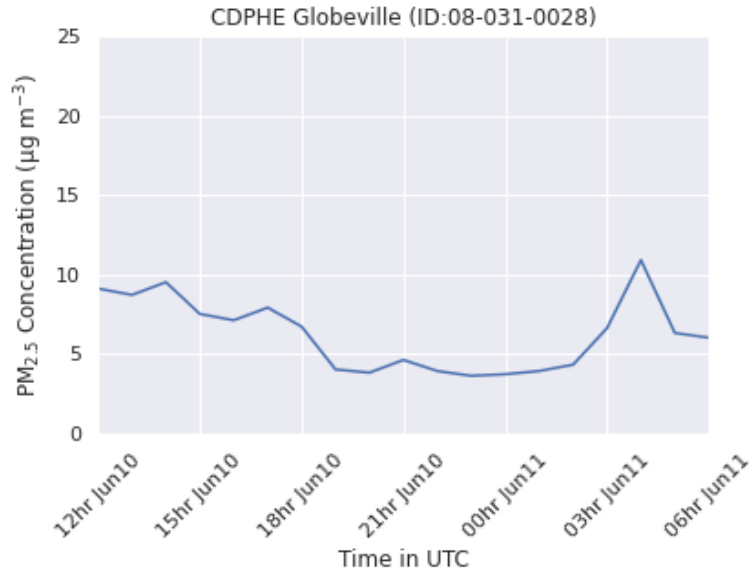


Figure 3.6 CDPHE Adams-Birch station PM_{2.5} observed hourly through the study period from 1200 UTC on 10 June 2022 to 0600 UTC on 11 June 2022 (0600 MDT on 10 June 2022 to 0000 MDT on 11 June 2022).



Figure 3.7 CDPHE La Casa NCORE (EPA AQS ID: 08-031-0026) station PM_{2.5} observed hourly through the study period from 1200 UTC on 10 June 2022 to 0600 UTC on 11 June 2022 (0600 MDT on 10 June 2022 to 0000 MDT on 11 June 2022).

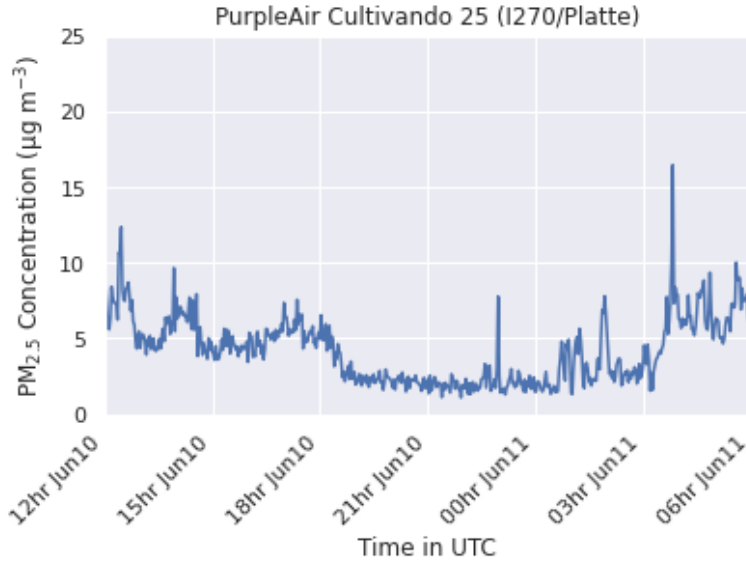


Figure 3.8 PurpleAir Cultivando 25 (I-270 and Platte River) station PM_{2.5} observed at two-minute resolution through the study period from 1200 UTC on 10 June 2022 to 0600 UTC on 11 June 2022 (0600 MDT on 10 June 2022 to 0000 MDT on 11 June 2022).

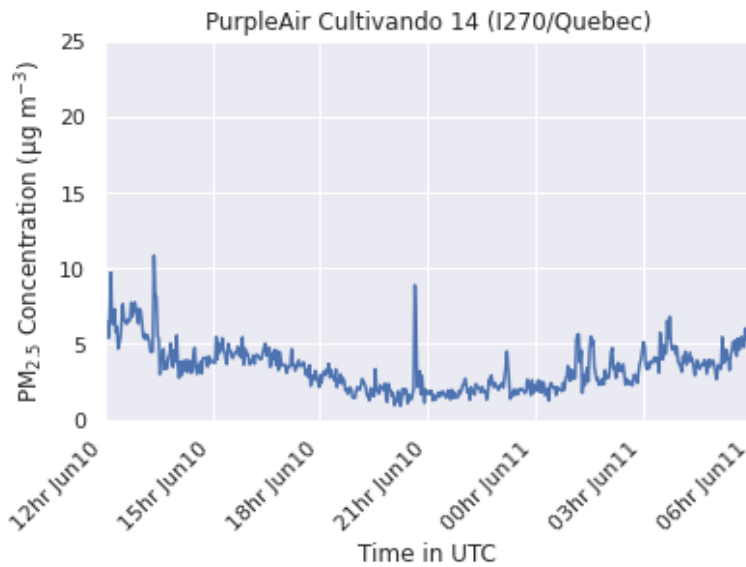


Figure 3.9 PurpleAir Cultivando 14 (I-270 and Quebec Street) station PM_{2.5} observed at two-minute resolution through the study period from 1200 UTC on 10 June 2022 to 0600 UTC on 11 June 2022 (0600 MDT on 10 June 2022 to 0000 MDT on 11 June 2022).

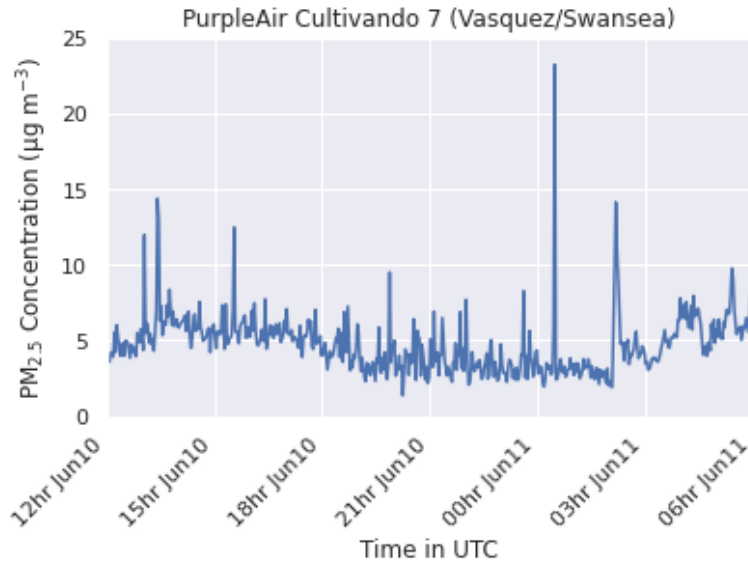


Figure 3.10 PurpleAir Cultivando 7 Vasquez and Swansea site PM_{2.5} observed at two-minute resolution through the study period from 1200 UTC on 10 June 2022 to 0600 UTC on 11 June 2022 (0600 MDT on 10 June 2022 to 0000 MDT on 11 June 2022).

Model Bias Evaluation

Given the temporal resolution, only the EPA reference sites are compared to the model simulations (Figures 3.11–3.13). Across all of the sites, the model simulation exhibits a low bias relative to the observed PM_{2.5} emissions. This is likely due to the model’s coarse vertical grid spacing (30 m) near the surface. The model is averaging emissions across too large a vertical area resulting in low simulated concentrations. However, as the model spins up (i.e., the time it takes to reach equilibrium given an initial forcing or perturbation) it does show a slight increasing trend similar to that observed from the EPA reference stations. While the magnitude is not well-aligned, the trend similarities are noteworthy. This discrepancy identifies a fruitful opportunity for future model refinement – adding very fine vertical grid cell spacing near the surface. That refinement is beyond the scope of this pilot study.

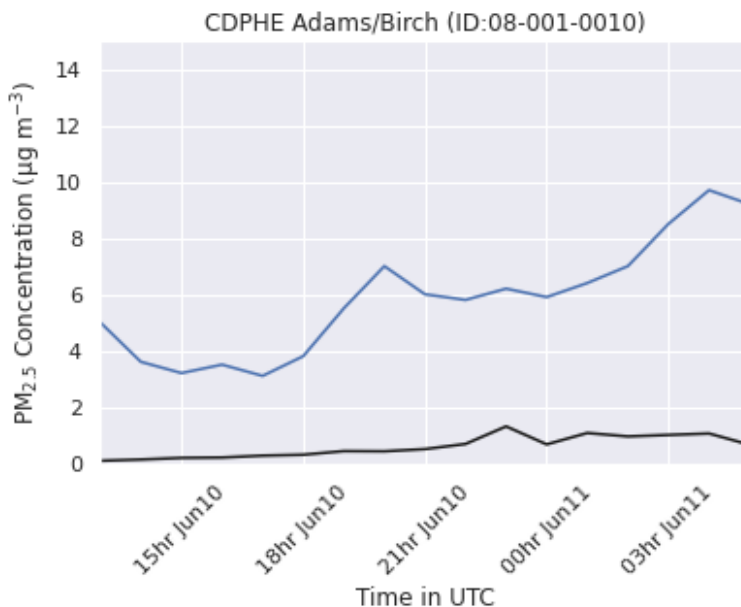


Figure 3.11 Adams Birch EPA site PM_{2.5} observed hourly (blue/top line) and WRF-Chem-LES simulation output (black/bottom line) through the study period from 1200 UTC on 10 June 2022 to 0600 UTC on 11 June 2022 (0600 MDT on 10 June 2022 to 0000 MDT on 11 June 2022).

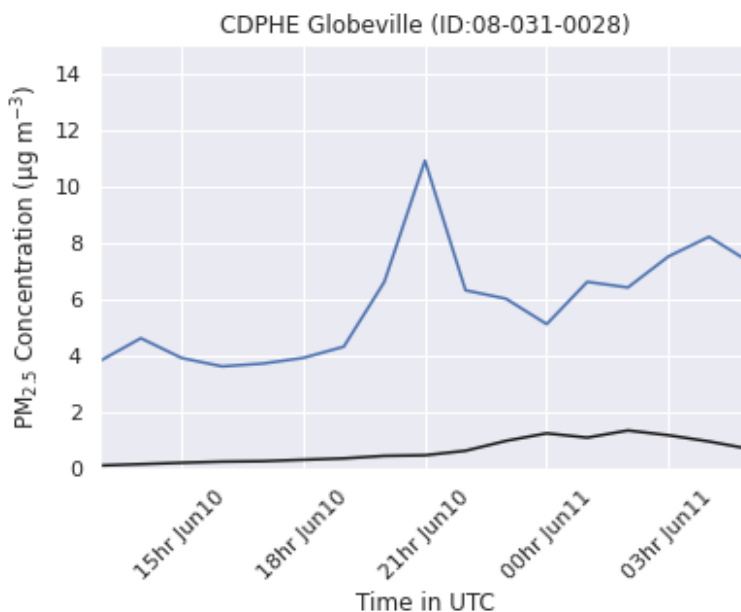


Figure 3.12 Globeville EPA site PM_{2.5} observed hourly (blue/top line) and WRF-Chem-LES simulation output (black/bottom line) through the study period from 1200 UTC on 10 June 2022 to 0600 UTC on 11 June 2022 (0600 MDT on 10 June 2022 to 0000 MDT on 11 June 2022).

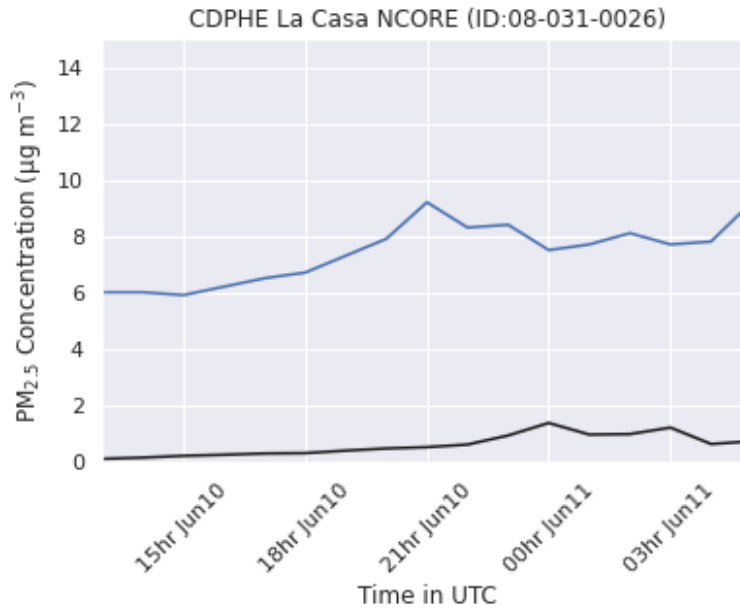


Figure 3.13 La Casa NCORE EPA site PM_{2.5} observed hourly (blue/top line) and WRF-Chem-LES simulation output (black/bottom line) through the study period from 1200 UTC on 10 June 2022 to 0600 UTC on 11 June 2022 (0600 MDT on 10 June 2022 to 0000 MDT on 11 June 2022)

Air Quality Heat Maps

The model simulated concentrations of construction emissions of PM_{2.5} along the corridor are visualized with a “heat map” of the ratio of construction emissions to total emissions averaged over the simulation period. In the outer domain (Figure 3.14), construction emissions are clearly visible along the corridor, where the 30% enhanced emissions were added and account for up to 5% of the total PM_{2.5} concentration in some areas. As emissions for the construction tracer were input from a line source along the roadways, the area of influence shows the impacts of downstream transport of these emissions. To better visualize how this proof-of-concept model can be applied as a stakeholder-relevant tool, results from the higher resolution inner domain have been plotted and overlayed on a street map for the I270 corridor (Figure 3.15). Here we can once again see the emissions well-represented along the corridor and into the surrounding neighborhoods.

Proxy emissions from construction activity were derived from national-scale highway shapefiles and as such, do not match the model lat-lon projection. This mismatch results in differences in the location of construction emissions for domains d01 and d02 and in turn the elevated levels of construction related air quality seen in the northeast corner of Figure 3.15. Future work is planned to better resolve inconsistencies in matching administrative boundaries with model domains and projections.

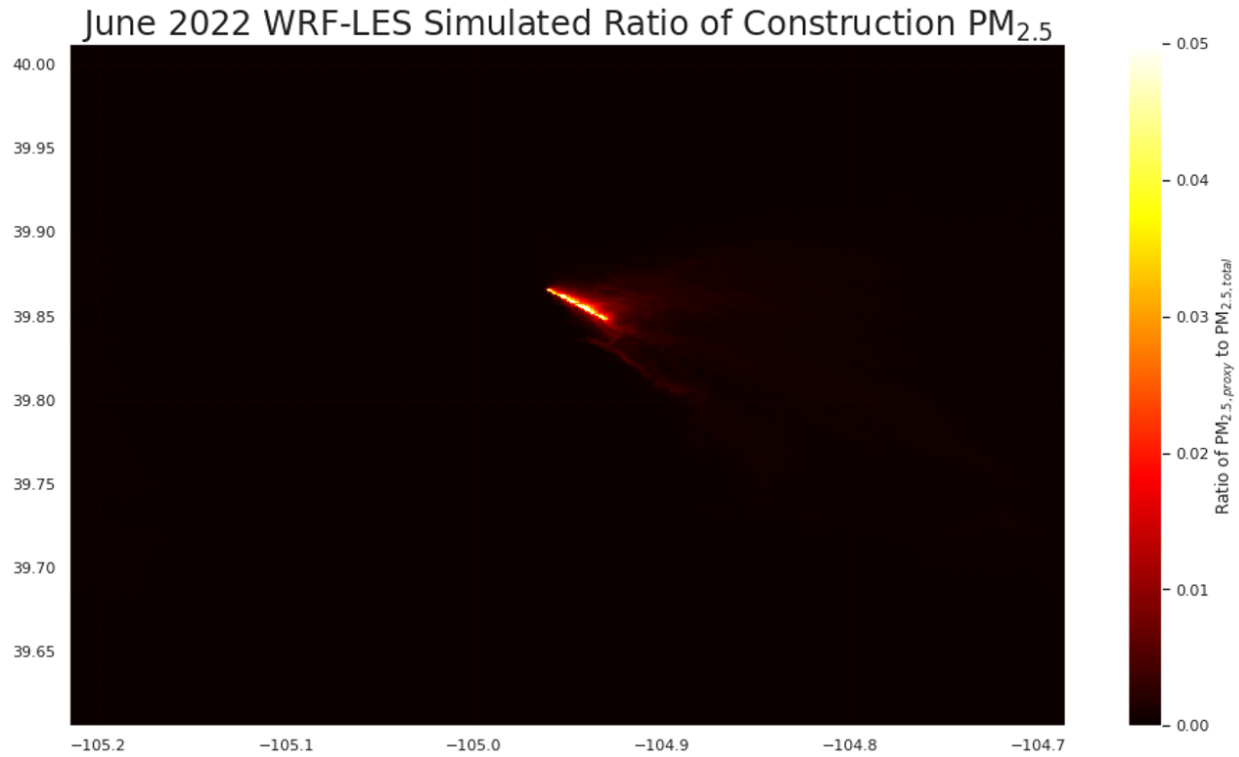


Figure 3.14 Ratio of PM_{2.5} construction emissions to total PM_{2.5} emissions along the corridor from WRF-Chem-LES simulations across the outer domain (d01) through the study period from 1200 UTC on 10 June 2022 to 0600 UTC on 11 June 2022 (0600 MDT on 10 June 2022 to

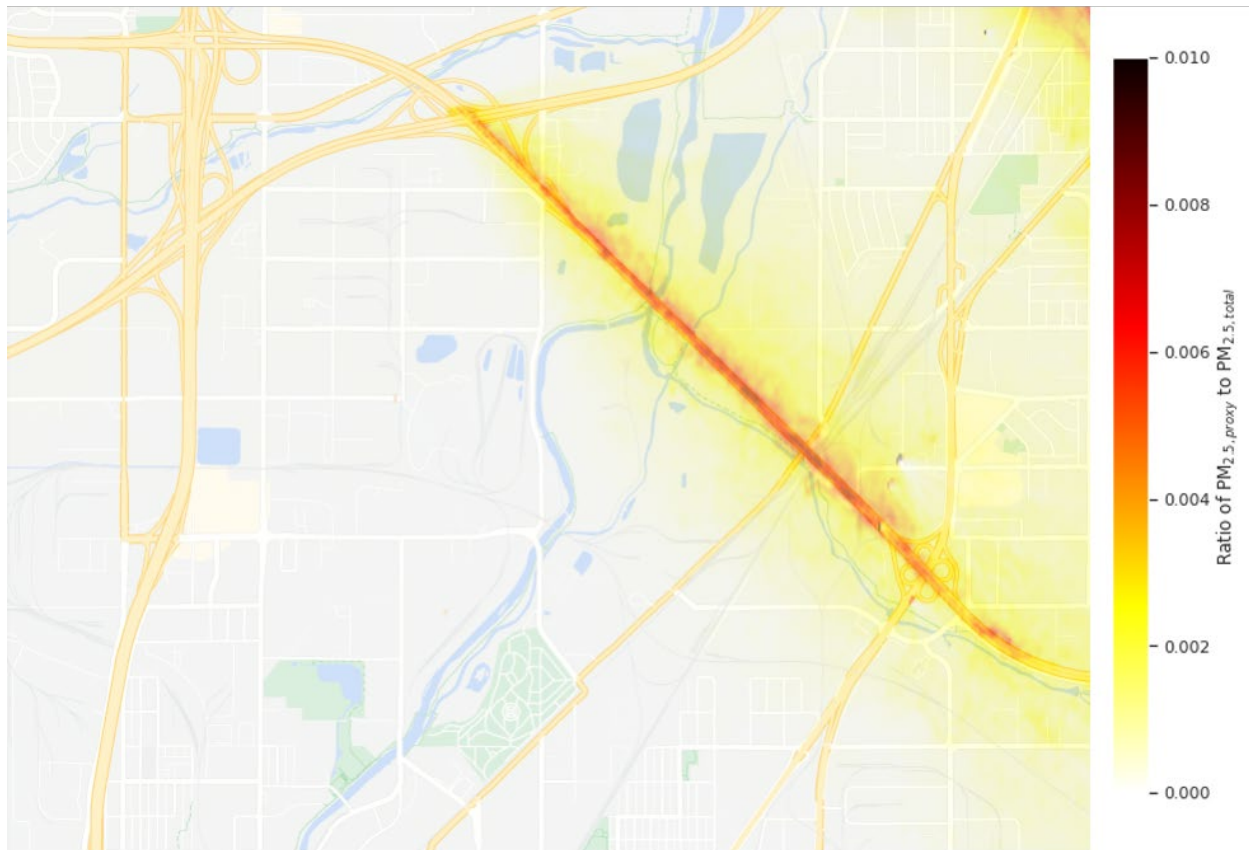


Figure 3.15 Proof-of-concept representation of the WRF-Chem-LES simulations across the inner domain (d02) through the study period from 1200 UTC on 10 June 2022 to 0600 UTC on 11 June 2022 (0600 MDT on 10 June 2022 to 0000 MDT on 11 June 2022) over the I-270 highway to show dispersion from the line source of emissions.

3.3 Low-Cost Sensor Analysis

In conjunction with the WRF-LES modeling results, the work presented here aims to understand the use and value of the deployment of low-cost sensors for quantifying the impact of road and near-road activity on ambient air quality. Low-cost sensors are defined by the EPA as observational units costing less than 2500 USD per unit. As shown in Figure 1.2, the study region for this analysis includes the network of low-cost sensors owned and operated by CDOT (Clarity Node-S and Lunar Outpost Canary-S) along the corridor, and a more dispersed network of PurpleAir low-cost sensors operated by a Colorado non-profit. All of these instruments are widely used for evaluating ambient air quality.

For the time period, the PurpleAir sensors, in general, have a lower range of observational variability (Figure 3.16) due to the larger number of observations (2-minute sampling versus 1-hour average). Standard deviations were computed across all sensors for each manufacturer over the period. The sensors closer to the roadways (Clarity and Lunar Outpost) tend to have higher concentrations of PM_{2.5} because of their proximity to highway emissions.

A fairly direct comparison of these low-cost sensor models is shown using the cluster of sensors

near I-270 and the Sand Creek Greenway (Figure 3.17). The magnitude and diurnal trend of each of these sensors agrees with prevailing traffic patterns and elevated pollution during the morning and evening rush hours, with the highest concentrations in the morning when the atmospheric boundary layer is most shallow, trapping emissions near the surface rather than diluting them through a deeper vertical layer.

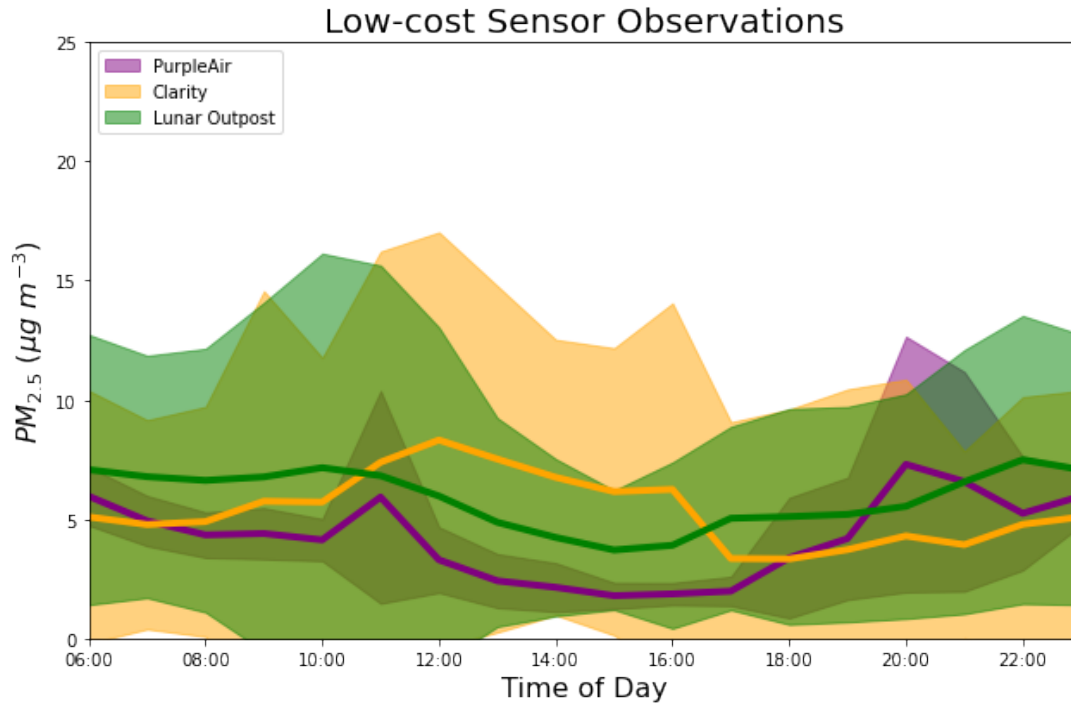


Figure 3.16 Low-cost PM_{2.5} sensors within the high-resolution spatial and temporal model domain (Figures 1.2 and 2.1) showing the hourly mean +/- one standard deviations.

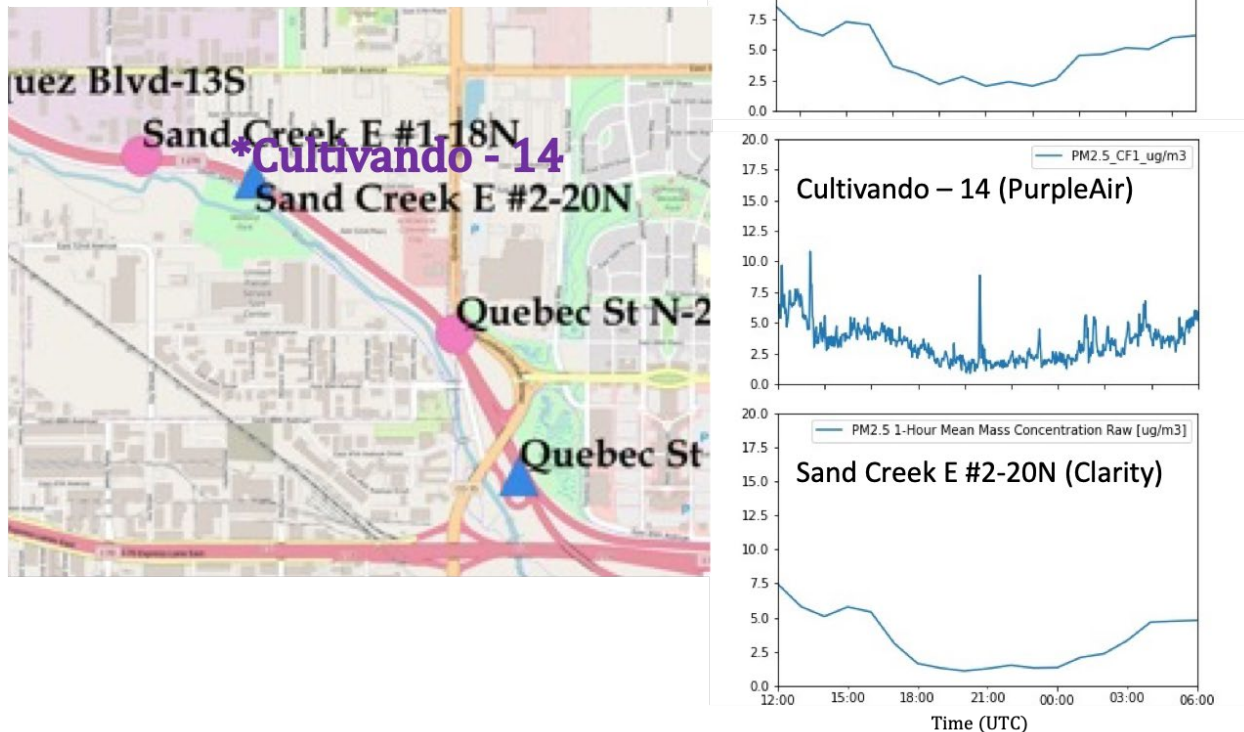


Figure 3.17 Co-located sensors and their time series along the I-270 corridor.

Several successful methods for bias correction (calibration) of PM_{2.5} from low-cost sensors have been demonstrated in the literature, generally based on correcting for effects of atmospheric relative humidity and temperature (e.g., Barkjohn et al. 2021; deSouza et al. 2022). A goal of this pilot study was to add high-resolution model data to supplement the other data sources for low-cost sensor bias correction. However, this goal was beyond what the study duration and resources allowed, and it may be pursued in future work, as discussed in section 4.

3.4 Study Limitations

As a pilot study, this work was limited in scope. The following limitations also represent opportunities for future exploration and improvement.

1. While the WRF-Chem-LES simulations included chemical tracers, the model was run in a quasi-idealized configuration without chemically active constituents. The model is capable of including reactive effects, but with a higher computational cost.
2. The simulations were run for only a single day. We anticipate that the results for this day are reasonable and representative of days with quiescent large-scale forcing conditions. The model can be run with a more constrained idealized setup (e.g., imposing large-scale nudging including advective tendencies) or a real forcing setup (e.g., initial and lateral

boundary conditions from a higher-resolution model and/or reanalysis dataset) to provide a more accurate representation of the atmosphere on a specific day.

3. Vehicle-induced turbulence and dust entrainment were not explicitly considered. As described in the literature (e.g., Eskridge and Hunt 1979; Gordon et al. 2012), vehicle wake turbulence can be an important consideration in air quality and construction emissions analyses. However, it is also a complex undertaking given factors such as vehicle speeds, antecedent atmospheric conditions, total amounts of dust, and local turbulent dynamics. One potential method for future exploration includes parameterizing dust entrainment and dispersion downstream of construction activities. This may also require an observational study to provide further guidance and/or verification of parameterizations that may be developed. Local wind and turbulence conditions will influence how much of the dust transported by vehicles is dispersed and in which direction.
4. Surface roughness parameters were not optimized along the corridor to simulate additional drag from structures and/or proposed sound barriers. Also, PM10 concentrations were not analyzed in this study. Both limitations were due to time and computing resource constraints. Mao et al. (2013) explored some of the influence of shelterbelt on dust dispersion while Pournazeri and Princevac (2015) more explicitly considered sound barrier effects on air quality. These earlier studies provide a foundation for future investigation with the WRF-Chem-LES modeling framework.

Last, and perhaps most important for the modeling framework development, is the fact that there was no actual construction activity occurring along the corridor during the study period. Emissions and other parameters were tuned in consultation with CDOT and CDPHE. As construction in the corridor commences and measurements are collected, there can be opportunities for modeling real-world cases of construction emissions. This would provide insight into both the dispersion of the emissions and the model capabilities and limitations.

4 Conclusions and Opportunities

Although a pilot study with limited scope, this work has demonstrated the application of the WRF-Chem-LES modeling framework in support of understanding roadway construction emissions. PM_{2.5} emission concentrations were successfully simulated along the corridor. The following model performance insights are found from comparison with surface observations of PM_{2.5}.

1. Overall, comparison with in-situ surface observations show the model values to have a significant low bias. This is likely due to the vertical extent of the lowest model grid level. This level thickness is large compared to the observation height. To improve the comparison, finer vertical resolution should be considered in future model simulations.
2. Temporally, the model simulations did show a gradual increase in concentration through the study period and a similar increase was present in observations. This increase may be indicative of reduced turbulent convective conditions once daytime heating ends, as well as the apparent wind direction shift and subsequent emissions transport from beyond the study area.
3. The model simulations did not capture the occasional, brief peaks in concentration observed by the high temporal resolution low-cost sensors. This is expected because the

sensors make point measurements, and the model has inherent averaging within grid cells.

Overall, these results demonstrate the potential for model simulations to provide an understanding of localized, construction-related air quality emissions including their horizontal and vertical transport.

This study also suggests many opportunities for further development of the model for construction air quality uses, and for its application more generally to transportation air quality research questions. Simple extensions of computation and analysis would extend the work to understand the effects of reactive chemistry and of the settling of larger particulates. Further work could address the limitations described in section 3.4. Specifically, there are opportunities to consider vehicular dust entrainment, explicit model tracers for PM₁₀, modification of surface roughness parameters, and ensuring inputs contain actual construction activity.

An additional direction of investigation could be to assess the value of coupling the WRF-Chem-LES modeling framework with the EPA Motor Vehicle Emissions Simulator (MOVES; EPA 2022). This would allow for a more detailed assessment of vehicular emissions in the context of atmospheric and chemical dynamics.

A further application of the WRF-Chem-LES model would be to evaluate the value of specific placements and networks of monitors. For example, in Chicago, Illinois and Salt Lake City, Utah municipalities have placed fixed and mobile sensors on public transit and transit infrastructure such as bus shelters (Ashcraft 2021; Spencer 2021). Given Colorado's public transit services such as CDOT's recently expanded Bustang service (including Pegasus) as well as locally operated transit, there is potential for broad fixed and mobile monitoring observations throughout the state. Modeling could help evaluate the cost and benefit of such observations.

5 References

- Ashcraft, E., 2021: UTA electric buses being outfitted with air quality monitors for better data, better policies. Accessed 21 November 2022. Available online at <https://www.ksl.com/article/50258520/uta-electric-buses-being-outfitted-with-air-quality-monitors-for-better-data-better-policies>.
- Barlow, J.F., 2014: Progress in observing and modelling the urban boundary layer. *Urban Climate*, **10**, 216–240, doi: 10.1016/j.uclim.2014.03.011.
- Barkjohn, K.K., B. Gantt, and A.L. Clements, 2021: Development and Application of a United States Wide Correction for PM_{2.5} Data Collected with the PurpleAir Sensor. *Atmospheric Measurement Techniques*, **14**, 4617–4637, doi: [10.5194/amt-2020-413](https://doi.org/10.5194/amt-2020-413).
- CDOT, 2022: I-270 Corridor Improvements. Accessed 21 November 2022. Available online at <https://www.codot.gov/projects/i270>.
- deSouza, P., R. Kahn, T. Stockman, W. Obermann, B. Crawford, A. Wang, J. Crooks, J. Li, and P. Kinney, 2022: Calibrating Networks of Low-Cost Air Quality Sensors. *Atmospheric Measurement Techniques Discussions*, **15**, 6309–6328, doi: [10.5194/amt-2022-65](https://doi.org/10.5194/amt-2022-65).
- Durant, J.L., C.A. Ash, E.C. Wood, S.C. Herndon, J.T. Jayne, W.B. Knighton, M.R. Canagaratna, J.B. Trull, D. Brugge, W. Zamore, and C.E. Kolb, 2010: Short-term variation in near-highway pollution gradients on a winter morning. *Atmos. Chem. Phys.*, **10**, 5599–5626.
- EPA, 2021: 2017 National Emissions Inventory (NEI) Data, January 2021 version. Accessed 29 November 2022. Available online at <https://www.epa.gov/air-emissions-inventories/2017-national-emissions-inventory-nei-data>.
- EPA, 2022: Latest Version of Motor Vehicle Emission Simulator (MOVES). Accessed 21 November 2022. Available online at <https://www.epa.gov/moves/latest-version-motor-vehicle-emission-simulator-moves>.
- Eskridge, R.E., and J.C.R. Hunt, 1979: Highway Modeling. Part I: Prediction of Velocity and Turbulence Fields in the Wake of Vehicles. *Journal of Applied Meteorology*, **18**, 387–400.
- Gordon, M., R.M. Staebler, J. Liggio, P. Makar, S. Li, J. Wentzell, G. Lu, P. Lee, and J.R. Brook, 2012: Measurements of Enhanced Turbulent Mixing near Highways. *Journal of Applied Meteorology and Climatology*, **51**, 1618–1632, doi: 10.1175/JAMC-D-11-0190.1.
- Grell, G.A., S. E. Peckham, R. Schmitz, S.A. McKeen, G. Frost, W.C. Skamarock, and B. Eder, 2005: Fully coupled “online” chemistry within the WRF model. *Atmospheric Environment*, **39**, 6957–6975, doi: 10.1016/j.atmosenv.2005.04.027.

- Heist, D.K., S.G. Perry, and L.A. Brixey, 2009: A wind tunnel study of the effect of roadway configurations on the dispersion of traffic-related pollution. *Atmospheric Environment*, **43**, 5101–5111, doi: 10.1016/j.atmosenv.2009.06.034.
- Hersbach, H., B. Bell, P. Berrisford, S. Hirahara, A. Horányi, J. Muñoz-Sabater, J. Nicolas, C. Peubey, R. Radu, D. Schepers, A. Simmons, C. Soci, S. Abdalla, X. Abellan, G. Balsamo, P. Bechtold, G. Biavati, J. Bidlot, M. Bonavita, G. De Chiara, P. Dahlgren, D. Dee, M. Diamantakis, R. Dragani, J. Flemming, R. Forbes, M. Fuentes, A. Geer, L. Haimberger, S. Healy, R.J. Hogan, E. Hólm, M. Janisková, S. Keeley, P. Laloyaux, P. Lopez, C. Lupu, G. Radnoti, P. de Rosnay, I. Rozum, F. Vamborg, S. Villaume, J.-N. Thépaut, 2020: The ERA5 Global Reanalysis. *Quarterly Journal of the Royal Meteorological Society*, **146**, 1999–2049, doi: [10.1002/qj.3803](https://doi.org/10.1002/qj.3803).
- Jiménez, P.A., J. Dudhia, J.F. González-Rouco, J. Navarro, J.P. Montávez, and E. García-Bustamante, 2012: A Revised Scheme for the WRF Surface Layer Formulation. *Monthly Weather Review*, **140**, 898–918, doi: 10.1175/MWR-D-11-00056.1
- Kunzli, N., R. Kaiser, S. Medina, M. Studnicka, O. Chanel, P. Filliger, M. Herry, F. Horak, V. Puybonnieux-Textier, P. Quénel, J. Schneider, R. Seethaler, J. Vergnaud, H. Sommer, 2000: Public-health impact of outdoor and traffic-related air pollution: a European assessment. *The Lancet*, **356**, 795–801, doi: 10.1016/S0140-6736(00)02653-2.
- Liu, Y., T. Warner, Y. Liu, C. Vincent, W. Wu, B. Mahoney, S. Swerdlin, K. Parks, and J. Boehnert, 2011: Simultaneous nested modeling from the synoptic scale to the LES scale for wind energy applications. *Journal of Wind Engineering and Industrial Aerodynamics*, **99**, 308–319, doi: 10.1016/j.jweia.2011.01.013.
- Loughner, C.P., D.J. Allen, D. Zhang, K.E. Pickering, R.R. Dickerson, and L. Landry, 2012: Roles of Urban Tree Canopy and Buildings in Urban Heat Island Effects: Parameterization and Preliminary Results. *Journal of Applied Meteorology and Climatology*, **51**, 1775–1793, doi: 10.1175/JAMC-D-11-0228.1.
- Mao, Y., J.D. Wilson, and J. Kort, 2013: Effects of a shelterbelt on road dust dispersion. *Atmospheric Environment*, **79**, 590–598, doi: 10.1016/j.atmosenv.2013.08.015.
- Pope III, C.A., and D.W. Dockery, 2012: Health Effects of Fine Particulate Air Pollution: Lines That Connect. *Journal of the Air & Waste Management Association*, **56**, 709–742, doi: 10.1080/10473289.2006.10464485.
- Pournazeri, S., and M. Princevac, 2015: Sound wall barriers: Near roadway dispersion under neutrally stratified boundary layer. *Transportation Research Part D*, **41**, 386–400, doi: 10.1016/j.trd.2015.09.025.
- Powers, J.G., J.B. Klemp, W.C. Skamarock, C.A. Davis, J. Dudhia, D.O. Gill, J.L. Coen, D.J. Gochis, R. Ahmadov, S.E. Peckham, G.A. Grell, J. Michalakes, S. Trahan, S.G.

- Benjamin, C.R. Alexander, G.J. Dimego, W. Wang, C.S. Schwartz, G.S. Romine, Z. Liu, C. Snyder, F. Chen, M.J. Barlage, W. Yu, and M.G. Duda, 2017: The Weather Research and Forecasting Model: Overview, System Efforts, and Future Directions. *Bulletin of the American Meteorological Society*, **98**, 1717–1737, doi: 10.1175/BAMS-D-15-00308.1.
- Ragland, K.W., and J.J. Peirce, 1975: Boundary Layer Model for Air Pollutant Concentrations Due to Highway Traffic. *Journal of the Air Pollution Control Association*, **25**, 48-51, doi: 10.1080/00022470.1975.10470049.
- Skamarock, W.C., J.B. Klemp, J. Dudhia, D.O. Gill, D. Barker, M.G. Duda, X.-Y. Huang, W. Wang, and J.G. Powers, 2008: A Description of the Advanced Research WRF Version 3. NCAR Tech Note No. NCAR/TN-475+STR, 113 pp., doi: 10.5065/D68S4MVH.
- Spencer, B., 2021: Chicago bus shelters monitor air quality. Accessed 21 November 2022. Available online at <https://www.itsinternational.com/its9/news/chicago-bus-shelters-monitor-air-quality>.
- Turner, B., 1970: Workbook of Atmospheric Dispersion Estimates. Environmental Protection Agency Publication No. AP-26. Accessed 16 November 2022. Available online at <https://nepis.epa.gov/Exe/ZyPURL.cgi?Dockey=9101S7UT.TXT>.
- Zimmerman, J.R., and R.S. Thompson, 1975: Users Guide for HIWAY: A Highway Air Pollution Model. Environmental Protection Agency Publication 165014-74-008, National Environmental Research Center 68 pp.